Photodeposition of metals from inks and their application in photocatalysis

Christopher O'Rourke, Nathan Wells and Andrew Mills*

School of Chemistry and Chemical Engineering, David Keir Building, Stranmillis Road, Belfast, BT18 9ET

andrew.mills@qub.ac.uk

Abstract

Films of Ag, Pt and Ag nanoparticles are photodeposited onto a range of commercial TiO_2 based photocatalytic materials, such as paint, tile, awning fabric and glass, as well as a TiO_2 sol-gel film, using an aqueous ink containing a sacrificial electron donor, glycerol, and the appropriate metal salt. The photodeposited metal films appear to be comprised of a fine covering of nanoparticular metal islands distributed evenly across the surface of the TiO_2 sol-gel film, with some large aggregated particles for Pt (106 nm) and Au (33 nm). The rate of deposition of Ag is particularly fast, since a 10 s exposure to 2 mW cm^{-2} UVA light produces a very noticeable colour change, which is ca. 60 times that of the other two metal-ion containing inks. When combined with a photomask, the metal inks are used to create finely detailed metal film images on the surfaces of a wide variety of different, mainly commercial, photocatalytic materials; a fine metal mesh photomask is used to make metal micro-patterns. When used to promote the photocatalysed oxidation of organic pollutants dissolved in aqueous solution, such as 4CP and MB, the enhancement in photocatalytic activity (compared to a plain TiO_2 film) exhibited by a photodeposited Pt on TiO_2 film is modest (16-35%), however, the enhancement is marked (234%) for the photocatalysed oxidation of CO to CO_2. In contrast, the Au and Ag films appear to depress the inherent activity of the naked TiO_2. The Pt/TiO_2 film also enhances significantly the photocatalysed oxidation of a film of soot (179%) but not of stearic acid (-23%); the Ag and Au films appear to impede the former reaction. The Pt/TiO_2 film exhibits the most significant enhancement in rate for the photocatalysed reduction of water to H_2 by ethanol, i.e. 62 times that of the Ag/TiO_2 film, which exhibits only a modest activity, which in turn is better than a naked TiO_2 film which shows no activity. The potential of the metal (ion) inks to more easily make photodeposited metal films on semiconductor photocatalyst films is discussed briefly.

Key words: photocatalyst; photodeposition; metals; platinum; inks; carbon monoxide; soot; hydrogen

Introduction

Environmental photocatalysis is a burgeoning area of research associated with many commercial products, such as photocatalytic glass, paints and tiles. In most cases the role of the semiconductor photocatalyst coating, which is almost always TiO_2, is to sensitise the oxidative mineralisation of ambient organic and inorganic pollutants, by ambient oxygen, i.e.

$$\text{Pollutant} + O_2 \xrightarrow[h\nu \geq E_{bg}]{TiO_2} \text{minerals (such as: } H_2O, CO_2 \text{ and acids)} \quad (1)$$

When the target pollutants are volatile organic carbons, VOCs, or NO_x, the commercial photocatalyst product is often promoted as being 'air-purifying' [1] and, in the case of organic and soot deposits, is usually advertised as being 'self-cleaning' [2]. Although the majority of commercial photocatalytic products are designed for air purification, or surface cleaning, photocatalysis is also a popular research area with regard to waste-water treatment [3] and the generation of potable water [4].

A commonly-employed approach to improve the performance of a semiconductor photocatalyst for reaction (1) is to deposit a catalyst, usually a platinum group metal which is most commonly platinum, Pt, onto its surface. The metal catalyst is believed to enhance the activity of the photocatalyst by: (i) acting as a sink for the photogenerated electrons (Schottky barrier electron trapping) and (ii) mediating the reduction reaction associated with the overall photocatalytic redox reaction [5]. Thus, in reaction (1), Pt 'islands' on the surface of a photocatalytic film or particle are reported [5, 6] to promote the reduction of O_2 by the photogenerated conduction band electrons, e^-, i.e.

$$O_2 + e^- \longrightarrow O_2^- \quad (2)$$

thereby leaving the photogenerated holes to oxidise the pollutant adsorbed on the surface of the semiconductor.

There are many different ways to effect metal deposition, including: the incipient wetness method (involving the thermal decomposition of a metal salt), electrodeposition, physical vapour deposition, metal colloid precipitation [7], chemical deposition (using a reducing agent) [5] and photodeposition (from metal salt solution) [5]. Of all these methods, photodeposition is the one most often employed since it is simple, inexpensive and usually creates very small metal islands (usually 2-4 nm diameter) which can enhance the activity of the photocatalyst for reaction (1) markedly (typically, the enhancement factor, δ, is 2-4) [6]. Note: here, δ is simply the ratio of the rate of the photocatalysed reaction with the metal-coated semiconductor photocatalyst to that of the naked photocatalyst.

The results of previous studies of reaction (1) suggest that an enhancement of 2-4 by a metal co-catalyst (usually Pt) on the surface of a photocatalyst (usually TiO_2) are most common for simple, low molecular weight pollutants, such as methanol, dichloroacetic acid and trichloroethylene [6]. In contrast, the kinetics for reaction (1) for large molecule pollutants, such as phenol and rhodamine 6G, are usually either enhanced only slightly (i.e. by < 50%), if at all or, depressed, i.e. exhibit negative % enhancement in rate and so a δ value < 1 [6].

In the photodeposition method, the photocatalyst, which is often in powder (or film) form, is dispersed (or immersed) in an anaerobic aqueous solution of the metal salt and illuminated with ultra-bandgap light. As a result, using a TiO_2 photocatalyst for example, the overall photodeposition reaction may be represented as follows:

$$nH_2O + 2M^{n+} \xrightarrow[h\nu \geq E_{bg}]{TiO_2} (n/2)O_2 + 2nH^+ + 2M\downarrow \qquad (3)$$

where, E_{bg} is the bandgap of the semiconductor photocatalyst (3.0 eV for anatase TiO_2). However, this approach often does not yield deposits of the metal, i.e. M^0, but rather deposits of one or more of its oxides, i.e. $M^{>0}$ [5]. For example, Xi *et al*, using anatase TiO_2 powder as the semiconductor photocatalyst and $PtCl_6^-$ as the metal salt, found that only $Pt(OH)_2$ was deposited in acid and neutral solution *via* the photocatalytic reaction (3) [8].

In contrast, when a sacrificial electron donor, i.e. SED, such as methanol [9], ethanol [10, 11] or glycerol [12], is added to the system, then usually – under acidic conditions at least - just the metal, i.e. M^0, is deposited upon irradiation. It has been suggested that the formation of M^0, is due in part to the highly reducing nature and action of the radicals formed when the SED is first oxidised by the photogenerated holes [10]. Thus, when an SED is present the overall photodeposition reaction may be summarised as follows:

$$n\text{SED} + M^{n+} \xrightarrow[h\nu \geq E_{bg}]{TiO_2} n\text{SED}^+ + M\downarrow \qquad (4)$$

Interestingly, although photodeposition often produces very effective photocatalysts, immersion of the photocatalyst and subsequent irradiation is not conducive to scale-up, which would be needed if such materials were to be commercialised. This feature, along with the material cost, provides a possible explanation as to why few, if any, commercial photocatalytic products utilise metal catalysts to improve their performance. It follows that any process that makes the photodeposition process easier would be a welcome advance.

In recent years this group has developed a number of different photocatalytic activity indicator inks, i.e. *paiis*, which, when coated onto the surface of a photocatalyst, change colour upon ultra-bandgap irradiation due to the photocatalysed irreversible reduction of a dye, typically resazurin, Rz, and concomitant oxidation of a SED, typically glycerol [13,14]. The overall photocatalytic process can be summarised as follows:

$$\underset{\text{(blue)}}{\text{Rz + glycerol}} \xrightarrow[\text{UV light}]{\text{TiO}_2} \underset{\text{(pink)}}{\text{Rf + glyceraldehyde}} \qquad (5)$$

where Rf is resorufin. Not surprisingly, the kinetics of reaction (5), a two electron process, is usually much faster than that for reaction (1) since the photomineralisation of most pollutants usually involves the transfer of many more electrons. For example, when the pollutant is methylene blue, MB, the complete oxidative mineralisation of one molecule requires the transfer of 102 electrons [15]! Thus, the complete photocatalytic reduction of an Rz ink, which is soon to become an ISO test [16], takes only ca. 10 min with Activ™ self-cleaning glass under a UV irradiance of 2 mW cm^{-2} (BLB light), whereas, with the same photocatalyst sample and irradiation conditions, the photomineralisation of a 10^{-5} M aqueous solution of MB takes ca. 30 times longer [17].

Although most work on *paiis* to date has focussed on using an easily and irreversibly reduced dye, such as Rz, to effect a colour change, there is no reason why ions of easily reduced metals, such as those of Ag, Pt and Au, might not be used instead. If effective, such a metal ion-containing ink could then be used to not only assess the photocatalytic activity of the underlying photocatalyst but also, and more importantly, as the basis of a simple, effective general route to photodeposit metal co-catalysts onto the surface of semiconductor photocatalysts. Since the photodeposition of metals from inks method is simple, and scalable, as inks can be readily printed, it follows that such an approach offers potential for the scaled-up production of metal-deposited photocatalyst films. In this paper, we describe the use of water-based metal-ion containing inks to effect the photodeposition of films of Ag, Pt or Au onto a number of different TiO_2-based, commercial photocatalytic coatings, as well as a sol-gel TiO_2 film. Here the metal films are photodeposited in templated patterns usually through the use of 'negative' masks and also assessed in terms of enhancement in photoactivity activity in a series of tests, which include the photo-oxidation of CO and soot.

Experimental

Materials

Unless stated otherwise all chemicals were purchased form Sigma Aldrich and used as received. The Aeroxide® P25 TiO_2 powder was a gift from Evonik (formerly

Degussa). Further details of the chemicals used to prepare the films are given below. All water used to make the aqueous solutions was doubly-distilled and deionised. All gases were purchased from BOC.

Commercial photocatalyst materials

A number of different commercial TiO_2-based photocatalytic materials were used as substrates for the photodeposition of metals (Ag, Pt and Au) from their salts dissolved in an aqueous ink, the details of which are given below. The different commercial photocatalytic substrates used were: tiles (Deutsche Steinzeug, [18]), paper (Mitsubishi Paper Mills; [19]), awning fabric (St. Gobain, [20]), and glass (Pilkington Glass; Activ™, [21]). Before the metal photodeposition process, all of these materials were first wiped clean with a damp cloth, and then irradiated with UVA radiation (two 8 W, blacklight blue (BLB) lamps with emission max of 352 nm; 4.0 mW cm^{-2}) for 2 h to ensure the surfaces were free from any surface organic contaminants.

The photocatalytic paint (Sto, StoColour Climasan; [1]) was coated onto a glass support (5 cm x 10 cm) using a doctor blade technique. Briefly, two strips of Scotch® Magic™ tape were placed at either side of the rectangular glass plate creating a 10 cm long, 60 μm deep trough. A line of paint was then syringed across the 5 cm top of the glass plate and drawn down using a glass rod, thereby creating a uniform coating of the paint which was then allowed to dry for 1 h before use, yielding a final (dry) thickness of 35 μm.

Sol-gel TiO_2 preparation

A paste of TiO_2 nanoparticles was prepared using a sol–gel method the details of which are described in detail elsewhere [22]. Briefly, an aliquot of the precursor solution, titanium(IV) isopropoxide (20cm^3), was modified through the addition of glacial acetic acid (4.65 g). The TiO_2 was then synthesised *via* the sol–gel process by the subsequent addition of 120 cm^3 of deionised water, containing 1.08 g of nitric acid, to the Ti(IV)/acetic acid solution, so as to generate a dispersion of the hydrous oxide. This dispersion was used to grow colloidal TiO_2 particles hydrothermally using an autoclave (220°C for 12 h). The resulting precipitated TiO_2 colloidal particles were then re-dispersed using an ultrasonic probe and then rotary evaporated until a weight percent of TiO_2 of 10–12% was achieved. At this point, 50 wt% of polyethylene glycol was added as a binder, to help prevent the formation of cracks when casting the paste to produce films, to yield a white paste final product, i.e. the 'sol-gel paste', which was mayonnaise-like in appearance and texture, and which, when coated in air, dries to form a clear film of amorphous TiO_2.

The sol-gel paste was cast onto glass microscope slides *via* the same doctor blade technique detailed above for coating the Sto paint and, after 30 min of drying, annealed at 450°C for 30 min with a ramp rate of 10°C min^{-1}. The film was then left overnight to cool slowly inside the furnace to create a final robust, clear coating of

anatase TiO_2 approximately 2 μm thick, which is referred to throughout as the 'TiO_2 sol-gel' film [22].

Metal-containing ink preparation

Ag, Pt, and Au inks were prepared according to a generic formulation involving the dissolution of metal salts in a 7.5 wt% of an aqueous solution of polyvinyl alcohol (i.e. PVA, MW = 124000 – 186000 g mol^{-1}). Thus, 2 g of glycerol were added to 20 g of the 7.5 wt% PVA solution and then 0.1 g the metal salt (i.e. $AgNO_3$, $H_2PtCl_6.6H_2O$ or $HAuCl_4$ (Alfa Aesar)) were added and the mixture left stirring in the dark for 1 h before being stored in a fridge for subsequent use. The pH of the Ag, Pt and Au inks were: 5.6, 2.5 and 2.8, respectively. In this work, for brevity, these inks are referred to as 'Ag, Au or Pt inks'.

Usually, the metal ink under investigation was applied to the range of photocatalytic surfaces using the doctor blade technique described above, which yielded air-dried ink films which were ca. 36 μm thick. In the photographic images work, the samples were irradiated through a photomask in order to provide the desired photodeposited metal film images. The mask was always an overhead transparency (Q-Connect®), onto which a black & white negative of the image required was printed.

Irradiations

Unless otherwise stated, all irradiations (i.e. photodeposition and photocatalytic) were performed using 2 x 8 W BLB's (Vilber Lourmat, λ_{max}(emission) = 352 nm), which provided an irradiance of 2.0 mW cm^{-2}. In all photodeposition experiments, after irradiating the sample, what remained of the metal-containing ink was washed off with water, so as to leave behind the photodeposited metal on the surface of the photocatalytic material under test. Unless stated otherwise, in all this work the irradiation times employed were: 10 s for the Ag ink and 10 min for Au and Pt inks. Figure 1 illustrates typical images of a photo deposited Ag, Pt and Au film on a 2.2 x 7.6 cm TiO_2 sol-gel film coated on a glass microscope slide.

Figure 1: Typical Ag, Pt and Au photodeposited metals on a sol-gel TiO_2 film, created using the standard metal inks, a UVA irradiance of 2 mW cm^{-2} and irradiation times of, 10 s (for Ag) and 10 min (for Pt and Au).

The typical photodeposited metal loadings for the films were determined (using ICP AAS) to be: 1, 1.6 and 0.6 wt %, for Ag, Pt, and Au with respect to TiO_2, respectively.

Methods

All UV/Vis spectra were recorded using a Cary 60 UV/Vis spectrophotometer. The scanning electron microscopy (SEM) studies were carried out using an FEI Quanta FEG Environmental SEM Oxford Ex-ACT instrument. In the study of the photoreduction of water, the evolution of H_2 was monitored using gas chromatography with a Shimadzu GC (GC-2014) which had a thermal conductivity detector (TCD) and a 5A molecular sieve column (Alltech CTR I, outer column 1/4" (molecular sieve), inner column 1/8" (porous polymer), stainless steel, 1.8 m long). The photocatalysed oxidation of CO was monitored using a Perkin Elmer Spectrum One FT-IR spectrometer, in which the sample under test was placed into an 10 cm gas cell (inner diameter = 2.8 cm) flushed with air, into which was injected 1 cm^3 of CO before irradiation. In this system, the sample under test was irradiated from below the gas cell, using a 10 W, 365 nm LED (from RS components), which generated a UV irradiance of 60 mW cm^{-2}. The photocatalytic destruction of 4-chlorophenol (4CP) and methylene blue, MB, were monitored using UV/Vis absorption spectroscopy with a Cary 60 UV/Vi spectrophotometer. The photo-oxidation of nitric oxide, NO, was monitored using a chemiluminescence gas analyser, (T200, Enviro Technology Services, UK). Throughout this work, all photographs were taken with a Cannon 7D MKII fitted with a 24-70 mm f2.8 II lens.

Results and Discussion

Film characterisation

The three typical metal-deposited films, on a TiO_2 sol-gel film, illustrated in figure 1 were subjected to a number of different characterisation studies. Scanning electron microscopy, SEM, using a conventional (i.e. non-high resolution) electron microscope yielded a clear image of the TiO_2 particles (average diameter: ca. 29 nm), as illustrated in figure 2(a), but no images of the metal particles, although Energy Dispersive Spectroscopy (EDS), performed in conjunction with SEM, shows that in each of the films illustrated in figure 1 the metals are finely dispersed over the surface of the TiO_2 film, but too fine to be resolved using a conventional (i.e. non-high resolution) SEM. This is not too surprising given that photodeposition, using an alcohol-based SED, generally yields metal particles with diameters of 2-4 nm [5]. Although the Ag-coated TiO_2 film looked very similar to that of the TiO_2 film alone, see figure 2(a), the Au-deposited film, figure 2(b), not only appeared to comprise a film of fine particle but also some larger ones (33 ± 5 nm), as illustrated by the white dots in the SEM in figure 2(b). In the case of the Pt-deposited film (figure 2(c)), even larger Pt particles were observed (106 ± 11 nm) but these were clearly clusters of

much smaller (21 ± 4 nm) particles of Pt shown in figure 2(d). The formation of Pt clusters has been observed by others using the photodeposition technique [12].

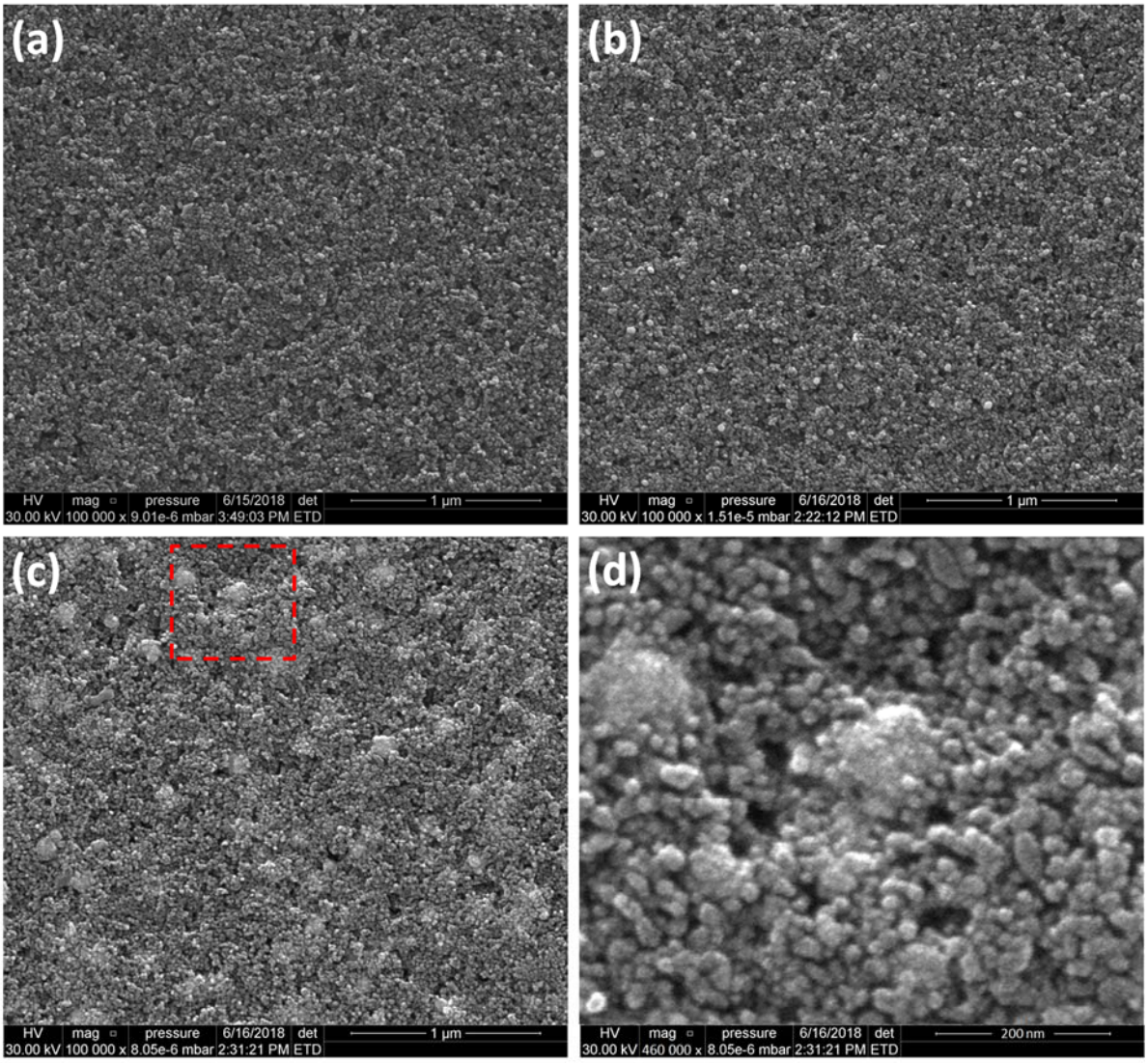

Figure 2: Scanning electron micrographs of: (a) TiO_2 particles that make up the TiO_2 sol-gel films used in this work (magnification 100,000) and images for the: (b) Au, and (c) Pt photodeposited films illustrated in figure 1. (d) Expanded view of the red box in (c) showing a Pt cluster (106 nm) comprised of small 21 nm Pt particles.

Each of the metals in the films illustrated in figure 1 were dissolved using aqua regia and the resulting solutions analysed using ICP-AAS to yield metal loadings of: 5, 3 and 8 $\mu g\ cm^{-2}$ for the Ag, Pt and Au films, respectively, which, assuming spherical geometry and an average diameter of 4 nm (i.e. the typical particle size reported for photodeposition of metals on the surface of TiO_2 [5], which could not be resolved in the SEM images in figure 2), indicates particle densities and nearest neighbour

distances of 1.4, 0.4 and 1.2 x10^{13} particles cm^{-2} and 2.7, 4.9 and 2.8 nm, for the Ag, Pt and Au films, respectively. This would explain why the EDS analysis of all the metal deposited films suggested that each was coated with a layer of very finely divided metal particles.

The colours of the photodeposited Au, Ag and Pt films illustrated in figure 1 are as expected for nanoparticles of these metals, since, only the former two have the dielectric properties necessary for strong surface plasmon resonance (SPR) effects in the visible, whereas, Pt's plasmonic ability is very low and weak and the little SPR it exhibits is in the far-UV [23]. The films illustrated in figure 1 are optically transparent and thus amenable to investigation using UV/Vis spectrophotometry. Figure 3(a) illustrates the UV/Vis absorption spectra of the Ag, Pt and Au films illustrated in figure 1, and show the characteristic SPR peaks of Ag (λ(max) = 430 nm) and Au (λ(max) = 550 nm) nanoparticles.

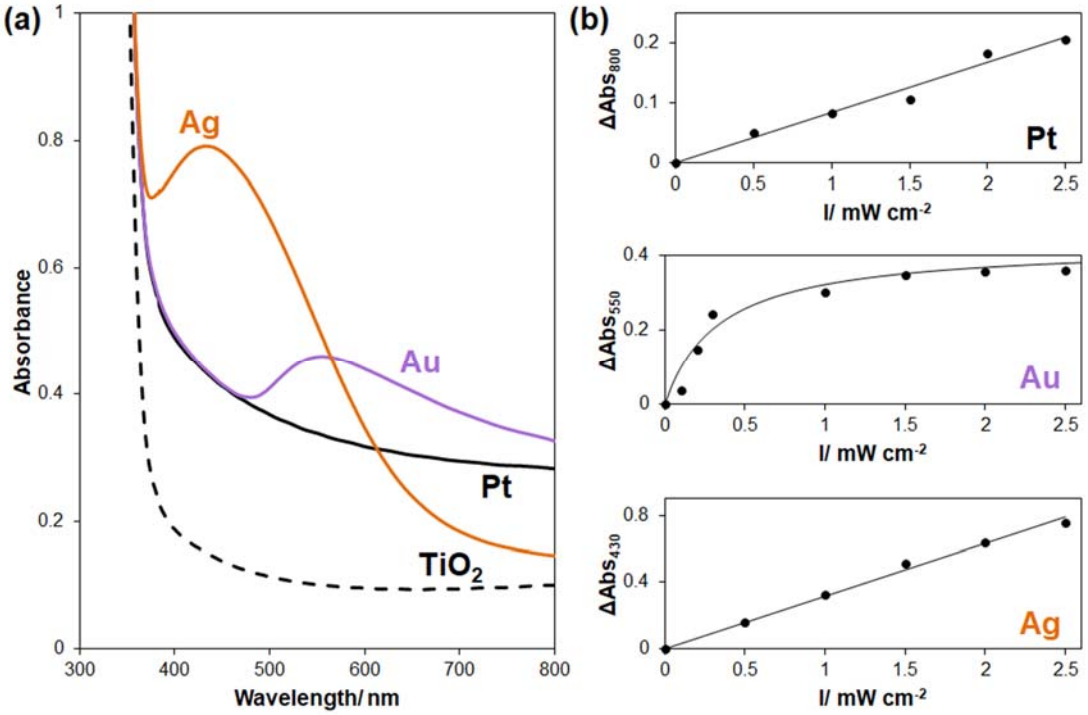

Figure 3: (a) UV/Vis absorption spectra of the Ag, Pt and Au photodeposited films illustrated in figure 1 and (b) absorbances of the Ag (at 430 nm), Pt (at 800 nm) and Au (at 550 nm) photodeposited films as a function of irradiance. The irradiation times used were 10 s for the Ag films and 10 min for the Pt and Au films.

In a series of simple experiments, using, respectively, irradiation times of: 10 s and 10 min for the Ag and (Pt and Au) inks, the *irradiance* used to photodeposit the metal films was varied, over the range 0-2.5 mW cm^{-2}, and the UV/Vis absorption spectra

of the resultant photodeposited Ag, Pt and Au films recorded. Interestingly, for each metal, the spectral profiles of the films were the same as those illustrated in figure 3(a), but the absorbance at λ(max) for the Ag and Au films, and, arbitrarily, 800 nm for the Pt films, increased, with increasing irradiance, as illustrated by the relevant absorbance vs irradiance plots shown in figure 3(b). The invariance in spectral profile shape (rather than magnitude) with irradiance suggests that the number, rather than size of the photodeposited particles increases with irradiance, which is also consistent with the linear dependence of absorbance vs irradiance illustrated in figure 3(b) for the Ag and Pt films. In striking contrast, however, the photodeposited Au film appears to show an initial linear dependence of absorbance with irradiance, which eventually levels off, so that at UV irradiances $\geq$ 1 mW cm^{-2} the UV/Vis absorption spectrum of the film did not change with increasing irradiance. The latter reslts suggest that at high irradiance (and fixed irradiation time), or long irradiances (and fixed irradiance level) the already photodeposited Au film impedes the further photodeposition of Au. An absorbance *vs* irradiation time profile for Au deposition on TiO_2, similar to that illustrated in figure 3, has been reported by others [24]. The reasons for this levelling off in Au photodeposition are unclear, although ultraband gap UV-screening of the underlying semiconductor by the photodeposited particles is likely to be a contributing factor.

Photocatalytic metal deposition patterning

As noted earlier, often the activity of the underlying photocatalysts can be improved by deposition a metal co-catalyst. It has been shown by others [25] that a large number of fine (12 μm) Au islands, rather than a few large square patches (2x2 mm), can improve markedly (2-5 times) the ability of n-CdS/p-CdTe photoanodes for water oxidation. This has inspired others to develop methods of micro or sub-micropatterning TiO_2 films using a photomask [26] or focussed laser beam [27], respectively. Others have demonstrated that a photomask approach can be employed to pattern photoelectrodes [28]. However, despite this early interest in patterning the surfaces of photocatalytic films, little subsequent research has followed. This lack of progress, exploring the efficacy of co-catalyst patterning of photocatalytic films, may in part, be due to the need to work with aqueous solutions of the metal salt, which is certainly a problem if scale up is required, however, as we shall see, it is one that can be readily overcome using a metal ion-containing ink instead.

In order to demonstrate efficacy of the metal inks described in this work for patterned film deposition on semiconductor films, a photocatalytic paint was used to cover three, 10x5 cm glass plates which were then covered with the Ag, Pt and Au inks as described in the experimental. A photomask, created from a photograph of one of the famous gantry cranes (named 'Goliath') which dominate the Belfast skyline [29], is illustrated in figure 4(a), and was used to cover each of the ink/paint glass plates

and the combination then irradiated with UV light (2 mW cm^{-2}) for the usual set period of time (i.e. 10 s for the Ag ink and 10 min for the Pt and Au inks). After irradiation, each plate was rinsed well with water to remove any remaining ink, so as to leave behind the photodeposited metal film created by irradiating through the negative 'Goliath' photomask. The resulting metal-on-photocatalytic-paint images for the Ag, Pt and Au inks are illustrated in figures 4(b-c), respectively and, in each case, the photocatalytic image reveals that much of the fine detail in the original photographic image, including the background clouds, has been captured by this simple photodeposition-through-a mask process.

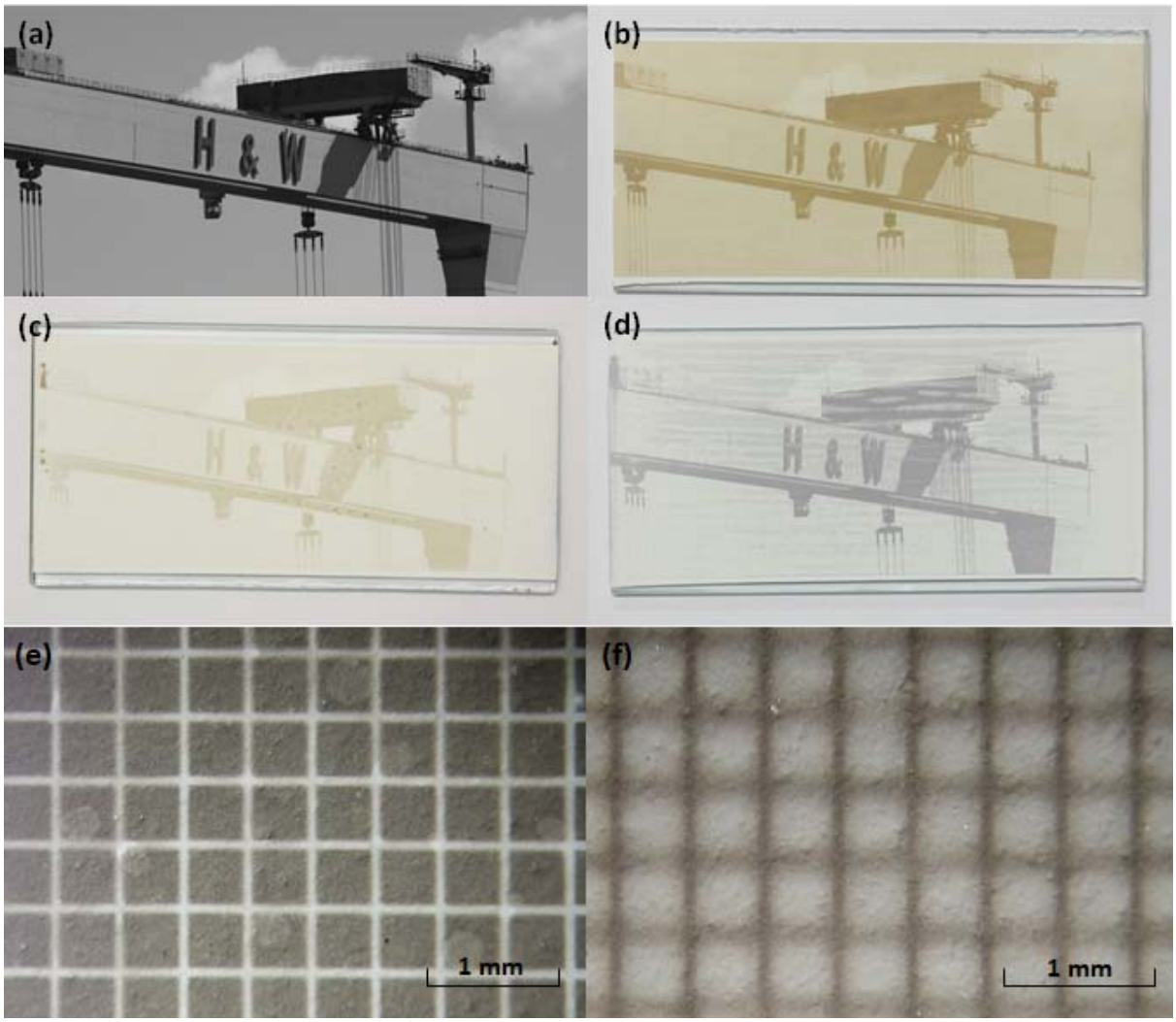

Figure 4: (a) original photograph and (b - c) photodeposited metal (on photocatalytic paint film) images of the 'Goliath' gantry crane on glass slides, where the metals deposited were: (b) Ag, (c) Pt and (d) Au. Figures (e) and (f) are photographs taken through a microscope, and were created using a Ni wire mesh (67 μm wires separated by 430 μm gaps) as the photomask on a Ag ink covered photocatalytic paint film. In all cases, the irradiation conditions and times were as reported in figure 1.

When a fine metal mesh is used instead as the photomask with the Ag ink, it is possible to generate a regular pattern of metal squares (470 μm) on a photocatalytic paint film, as illustrated by figure 4(d). In addition, when a negative of the metal mesh is used instead as the photomask, an Ag photodeposited metal image of the metal wires (67 μm thick) is generated, as illustrated in figure 4(e). The results of this work show that the metal ink technology demonstrated here provides a simple and easy to use approach to the micro-patterning of the surfaces of photocatalytic films.

In order to show that the ink film photodeposition method can be used to create metal films on other photocatalytic surfaces, a number of different commercial photocatalytic films and one lab-based film (a TiO_2 sol-gel film) were coated with the **Ag ink** and irradiated through a photomask negative image of the stained glass window in Queen's University Belfast, illustrated in figure 5(a). The resulting images for photocatalytic: sol-gel, paint, tile, paper, awning fabric and glass, are illustrated in figure 5(b).

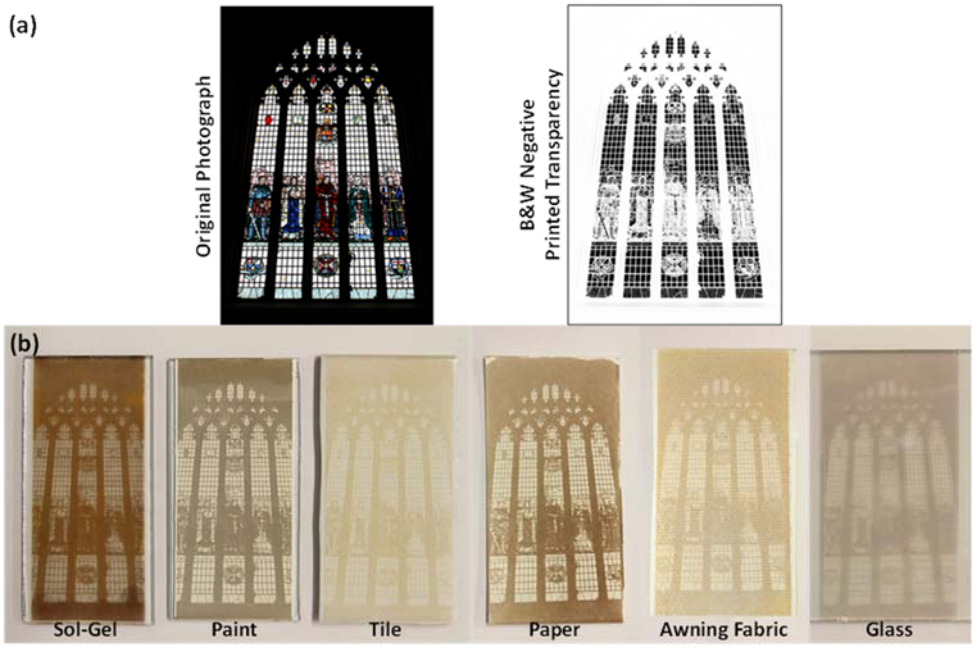

Figure 5: (a) Original photograph and negative image, used as photomask, of a stained glass window which was used to create the Ag photodeposited metal (on photocatalytic film) images on: sol-gel, paint, tile, paper, awning fabric and glass illustrated in (b). The irradiation conditions used were as described in figure 1, except that the irradiation times were: 0.1, 0.5, 20, 0.1, 0.5 and 10 min for the photocatalytic sol-gel, paint, tile, paper, awning fabric and glass substrates, respectively.

Other works show that the Pt and Au inks develop the same images, but using a longer irradiation time (10 min rather than 10 s). These results suggest that patterning, including micro-patterning is possible on a wide range of photocatalytic surfaces using the metal-ion based inks described in this work. In addition, the very rapid reduction of the Ag ink (60 times faster than the Pt and Au inks) suggests it would make a good, relatively inexpensive photocatalyst activity ink [14] and, although it would leave a semi-permanent metal deposit/mark on the surface under test, the metal can be removed by abrasion or treatment with a strong acid. Why the Ag ink is much easier to reduce photocatalytically than the Pt or Au inks is not clear, given the standard redox potentials for the Ag^+/Ag, $[PtCl_6]^{2-}/Pt$ and $[AuCl_4]^-/Au$ couples are: 0.80, 0.72, 1.0 V, respectively, although one possibility is that unlike the reduction of Ag^+, the reduction of $[PtCl_6]^{2-}$ and $[AuCl_4]^-$ to their respective metals are both multi-electron transfer processes which may require the generation of high energy intermediates and, by so doing, present a barrier to the overall electron transfer process that is not present in the one electrode reduction of Ag^+.

Photocatalytic oxidation: aqueous solution

As noted earlier, a popular approach to improve the activity of a photocatalyst for reaction (1) is to deposit a co-catalyst, such as Pt, in the form of a fine deposit of islands on the surface of the photocatalyst. However, also as noted previously, often the enhancement in activity, when compared to the performance of the photocatalyst without metal co-catalyst, is small or non-existent when the pollutant concerned is large and the overall number of electrons transferred per molecule is large. Evidence for the latter is provided here by a study of the photo-oxidation of 4-chlorophenol, 4CP, using the TiO_2 sol gel film, with and without photodeposited Pt. The photocatalytic film under test was incorporated into the face of a 1 cm quartz cuvette – which then acts as the photoreactor – as described in detail elsewhere [30]. Into this 1 cm cell photoreactor, 3 cm^3 of an aqueous, aerated solution of the pollutant under test (here 4CP, concentration = 2.5 x 10^{-4} mol dm^{-3} in 0.01 M $HClO_4$) were placed and stirred vigorously using a magnetic stirrer flea. The system was then irradiated with UVA radiation (15 mW cm^{-2} from a 365 nm LED) and the change in UV absorption spectrum of the 4CP recorded periodically as a function of irradiation time. From the subsequent plots of the data in the form of absorbance at λ_{max} for 4-CP (i.e. 225 nm) versus irradiation time, the times taken to reduce the initial concentration of the 4CP by 50%, i.e. $t_{1/2}$, were determined for the bare and platinised TiO_2 films, as 5.28 and 4.52 min, respectively, suggesting an enhancement factor, δ, of only 1.16, i.e. an enhancement of only 16%.

In addition, the same experimental proccedure was repeated using the commonly employed test pollutant, methylene blue, MB, (10^{-5} mol dm^{-3}), and yielded a δ value of 1.35, i.e. an enhancement of 35%. The $t_{1/2}$ and δ values arising from all this work and the irradiation conditions, are listed in Table 1, and show that, for these two test pollutants at least, the rate of reaction (1) in aqueous solution is improved, but not

markedly by the photodeposited Pt on the TiO_2 sol-gel film, which is consistent with the findings of others [6]. It is not clear if this general lack of a striking enhancement in aqueous solution for large pollutant molecules, such as 4-CP and MB, is also found when studying reaction (1) for the removal of gaseous pollutants and so this is investigated in the following section.

Table 1: Photocatalysed reactions studied using naked and metal coated TiO_2 sol-gel films: enhancement factors and photoreaction half-lives

	Enhancement Factor, δ			
	Platinum[a]	**Gold[a]**	**Silver[a]**	**None**
Photocatalytic Oxidation: Solution				
4-Chlorophenol[b]	**1.16** ($t_{1/2}$ = 4.52 min)	--	--	**1** ($t_{1/2}$ = 5.28 min)
Methylene Blue[b]	**1.35** ($t_{1/2}$ = 30.3 min)	--	--	**1** ($t_{1/2}$ = 41.1 min)
Photocatalytic Oxidation: Gas				
Carbon Monoxide[c]	**3.11** ($t_{1/2}$ = 42 min)	**0.66** ($t_{1/2}$ = 201 min)	**0.55** ($t_{1/2}$ = 244 min)	**1** ($t_{1/2}$ = 134 min)
Nitric Oxide[d,e]	**1.36** (NO conversion = 26%)	--	--	**1** (NO conversion = 19.1%)
Photocatalytic Oxidation: Solid				
Soot[f]	**2.79** ($t_{1/2}$ = 35 h)	**0.33** ($t_{1/2}$ = 298 h)[g]	**0.063** ($t_{1/2}$ = 1533 h)[g]	**1** ($t_{1/2}$ = 97 h)[g]
Stearic Acid[f]	**0.77** ($t_{1/2}$ = 27.9 min)	--	--	**1** ($t_{1/2}$ = 21.4 min)
Photocatalytic Reduction: Solution				
Water[h,i]	**62** (k_{H2} = 5.9 µmol min^{-1})	**19** (k_{H2} = 1.8 µmol min^{-1})	**1.0** (k_{H2} = 0.09 µmol min^{-1})	**0** (k_{H2} = 0 µmol min^{-1})

a Unless otherwise stated, the films were as in figure 1 with typical metal loadings on the TiO_2 sol-gel (0.5 mg cm^{-2}) of; 1.6, 0.6, and 1 wt % for Pt, Au, and Ag respectively.
b 365 nm LED (RS Components, LedEngin Inc LZ1-10UV00, 2.8 W), I = 15 mW cm^{-2}.
c 365 nm LED (RS Components, LedEngin Inc LZ4-44UV00-0000, 10 W), I = 60 mW cm^{-2}.
d 352 nm BLB lamp, 2 x 15 W (Sankyo Denki), I = 1 mW cm^{-2}.
e Photocatalyst films were produced using P25 and Pt-P25 (Pt loading = 0.2 wt%)
f 352 nm BLB lamp, 2 x 8 W (Vilber Lourmat), I = 2 mW cm^{-2}.
g Determined via extrapolation of decay curves.
h 200 W Xe-Hg lamp (Spectral Energy LPS251SR), I_{UVA} = 12 mW cm^{-2}.
i Enhancement factors calculated with respect to the lowest performing catalyst (Ag-TiO_2) as a naked TiO_2 film produced no H_2

Photocatalytic oxidation: gas phase pollutants

A good example of co-(metal) catalyst enhancement of photocatalytic reaction (1) for a gaseous pollutant is to be found using carbon monoxide as the test pollutant. Here the overall reaction is as follows:

$$2CO + O_2 \longrightarrow 2CO_2 \qquad (6)$$

Thus, in a study of the above reaction, photocatalysed by the sol-gel TiO_2 or metal/TiO_2 films, each of the metals on sol-gel films illustrated in figure 1 were placed inside an IR-gas cell filled with air, and then 1 cm^3 of CO was injected into the cell. For each sample under test, the cell was placed into an FT-IR spectrometer and the photocatalysed oxidation of CO to CO_2 monitored spectrophotometrically, as a function of irradiation time, *via* the disappearance of the IR absorbance peak due to CO (at 2120 cm^{-1} and 2171 cm^{-1}), and the concomitant generation of CO_2 (2341 cm^{-1} and 2360 cm^{-1}). For convenience, in this system, the photocatalytic sample was irradiated from below using a 365 nm LED, with an incident irradiance of 60 mW cm^{-2}. A typical set of FT-IT absorption spectra recorded for the system, using a Pt/TiO_2 film, as a function of irradiation time are illustrated in figure 6.

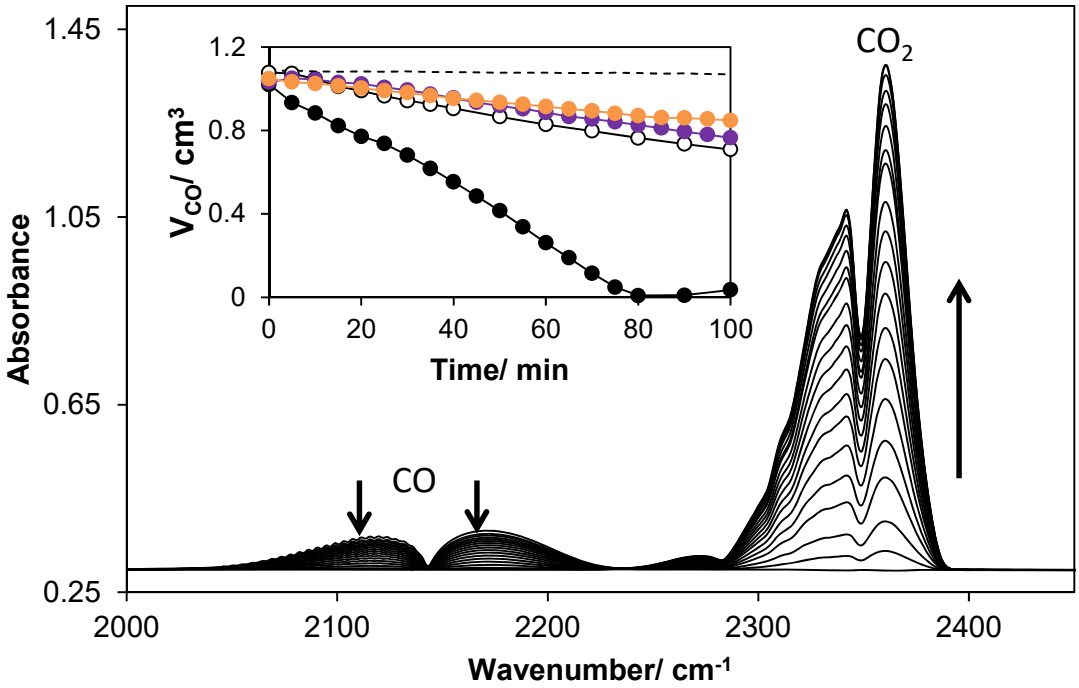

Figure 6: FT-IR absorbance spectra of a gas cell filled with air plus 1 cm^3 of CO and a Pt/TiO_2 sol-gel film, recorded every 5 min as a function of irradiation time; irradiance: 60 mW cm^{-1}. The insert diagram comprises plots of the volume of CO, V_{CO}, (derived from the measured absorbance at 2171 cm^{-1}) as a function of irradiation time for the (from bottom to top): Pt/TiO_2, TiO_2, Au/TiO_2 and Ag/TiO_2 films respectively. The horizontal broken line represents the plot of V_{CO} vs irradiation time for the system without any photocatalyst film present.

The absorbance peak due to CO, at 2171 cm^{-1}, was used to calculate the volume of CO, V_{CO}, remaining in the cell and the plots of V_{CO} vs irradiation time for the naked, Ag, Pt and Au TiO_2 are illustrated in the insert plot in figure 6. This data was then used to estimate the values of $t_{1/2}$ and δ for the TiO_2 and the Ag-, Pt- and Au-sol-gel TiO_2 films and the results are summarised in Table 1. A brief inspection of these results reveals that neither the Au, or Ag, photodeposited coating, enhance the activity of the TiO_2 sol-gel film towards the oxidation of CO to CO_2, indeed, they depress it, possibly due to the metal particles UV screening the underlying TiO_2 film. In contrast, the Pt co-catalyst produces a significant enhancement in activity (δ = 3.11, see Table 1). At first this may appear surprising, given that the overall process is a seemingly simple two electron transfer process and thus, as noted earlier, might be expected to show a significant enhancement, given the usual electrochemical model of photocatalysis usually employed by most researchers studying reaction (1) in aqueous solution, where Pt aids electron-hole separation and the reduction of O_2. However, this water-based electrochemical model is clearly inappropriate when discussing any gas phase versions of reaction (1), such as reaction (6) where, for example, the ambient environment is non-conducting and the adsorption conditions for reactants and products are so very different.

Work carried out by others [31, 32] on the photocatalysis of reaction (6) by TiO_2 suggests that CO adsorbs strongly onto Pt and is oxidised by an active oxygen species, O*, which is generated photocatalytically and may be O^- or O_3^- [32]. This mechanism is consistent with the lack of photocatalysis observed here for the TiO_2, Ag/TiO_2 and Au/TiO_2 films, as illustrated by the decay profiles in figure 6, given that the adsorption of CO on TiO_2, Ag and Au, is known to be much weaker than on Pt [33]. Further support for the above photocatalytic (rather than purely thermal) model for reaction (6), is the observation that in the dark, none of the materials are able to mediate reaction (6), as noted also by others [31,32].

The above results suggest that apparently stoichiometrically simple, gas phase reactions are most likely not that simple mechanistically and that the usual perceived roles of metal co-catalyst deposits based on an electrochemical model, namely: to promote the separation of photogenerated electrons and holes and to mediate reaction (2) as part of reaction (1), do not necessarily apply in the gas phase. Further evidence that this is the case is provided by the results of a study of the photo-oxidation of NO by O_2 to form HNO_3, i.e.

$$2NO + H_2O + 1.5O_2 \longrightarrow 2HNO_3 \qquad (7)$$

Previous work on the above reaction, photocatalysed by TiO_2, carried by this group [34] has established that, for all the commercial photocatalytic TiO_2 materials used here, as well as P25 TiO_2 powder-based films, prolonged irradiation leads to the accumulation of nitric acid on the surface of the photocatalyst which then mediates the simple conversion of NO to NO_2, i.e.

$$2NO + O_2 \xrightarrow{HNO_3} 2NO_2 \quad (8)$$

rather than reaction (7).

Interestingly, although reaction (7) is a well-studied photocatalytic process, few if any studies on reaction (7), and none on reaction (8), appear to have been conducted using metal-deposited films. Since on all the photocatalytic surface studied here, the desired removal of NO_x, i.e. reaction (7), eventually transforms into the undesirable oxidation of NO to NO_2, i.e. reaction (8), it was decided to see what effect photoplatinisation of the photocatalyst had on the latter reaction. Thus, a brief study of the photocatalysis of reaction (8) was carried out using a film of P25 TiO_2 with, and without, a photodeposit of Pt (0.2 wt%). The reaction was studied using the standard conditions and experimental set-up of the NO_X ISO, namely: 1 ppm NO in air, 50% RH, 3 dm^{-3} min^{-1}, irradiance: 1 mW cm^{-2} [35]. The two samples under test had already been photo-conditioned in the NOx reactor for 5 h in a stream of NO in order to generate sufficient HNO_3 on the surface of the photocatalyst so as to be sure that the only process under study was reaction (8). The results of this study revealed a %conversion of NO to NO_2 of 19.1 and 26.0% for the TiO_2 and Pt/TiO_2 films, respectively, which indicates an enhancement factor of 1.36, i.e. Pt has a modest but positive effect on the photocatalysed reaction (8).

The above results, on the CO and NO oxidation reactions, suggest that whilst in some cases a metal co-catalyst, like Pt, may markedly enhance the rate of reaction (1) in the gas phase, as in reaction (6) (δ = 3.11) in others, such as the oxidation of NO to NO_2 (δ = 1.36) the effect can be more modest.

Photocatalytic oxidation: solid pollutants

Although enhancement in photocatalytic rates by metal co-catalysts is well established for reaction (1), where the pollutant is either dissolved in aqueous solution, such as 4CP, or gaseous, such as CO, there appears to be little work on its effect on the photocatalytic mineralisation of solid pollutants – most probably because nobody expects there to be any enhancement, given the metal would be normally buried under a solid layer of the pollutant under test! However, for completeness, it was felt worthwhile to briefly investigate such systems using our Pt/TiO_2 and TiO_2 films, and the first system to be studied was that of the photocatalysed oxidation of a surface film of soot, i.e.

$$C + O_2 \longrightarrow CO_2 \quad (9)$$

Previous work by this group, and others [36-39], demonstrated that TiO_2 is able to photocatalyse reaction (9), albeit very slowly and inefficiently (the photonic efficiency of this process was estimated as: 1.1×10^{-4} [37]). In this initial study the metal film was photocatalytically deposited from a Pt ink which, instead of covering the whole TiO_2 film, was drawn down the centre of a TiO_2 film as a line, using the same

conditions as used to make the Pt film illustrated in figure 1. The soot was then deposited over the whole sample, i.e. over the thin Pt/TiO_2 line, the remaining naked TiO_2 film and glass boarders, by exposing it to the flame of a T-Light paraffin wax candle. SEM analysis of the soot film revealed it to be very fluffy in appearance – rather like candy floss - with a typical film thickness of ca. 3.5 μm. Photographs of a typical film before and after soot deposition are illustrated in figure 7. It follows that, upon UV irradiation of just this one sample, there will be three very different photocatalytic activities with regard to reaction (9) exhibited due to the three very distinct regions of the film, namely: (i) the Pt/TiO_2 film, (ii) the TiO_2 film, and (iii) the microscope glass. Thus, during just one irradiation of the whole film, it should be possible to assess the activities of these three different regions simultaneously. In this work the photocatalytic activity of any region was assessed *via* an analysis of the depth of colour of the soot film as revealed by the digital images taken of the soot-covered sample as a function of irradiation time. Recent work has shown that such colour analysis can provide an approximate colourimetric substitute for absorbance measurements [40]. Thus, the soot-covered film was irradiated with UV light (2 mW cm^{-2}) and the photocatalysed removal of the soot, *via* reaction (9), was photographed periodically. Figure 7 shows the appearance of the soot covered film before and after 50 h UVA irradiation.

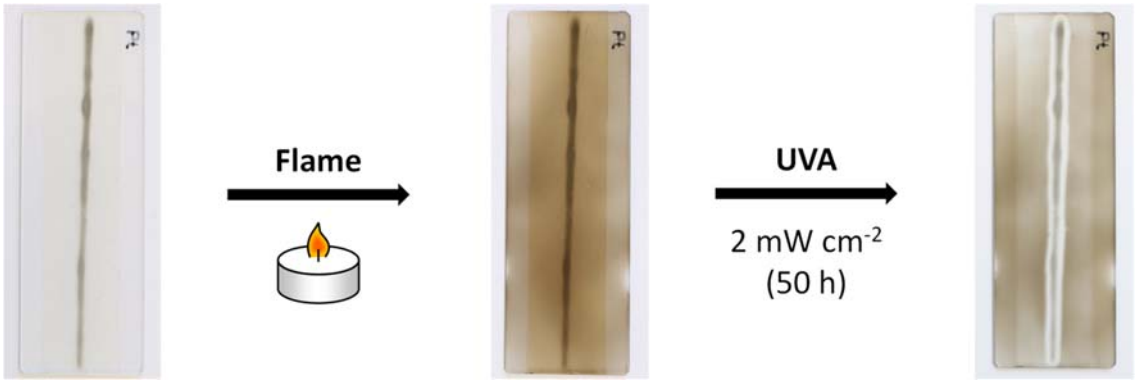

Figure 7: Digital photographs of a thin photodeposited Pt film, made using a Pt ink, on a TiO_2 sol-gel film, before and after covering with a thin layer of soot and then subsequent irradiation with UV light for 50 h.

From the images in figure 7 it is clear that both the TiO_2 and the Pt/TiO_2 films are able to effect the photocatalysed destruction of soot, whereas the glass substrate (i.e. the sample edges) are not. More importantly, the Pt/TiO_2 film appears to also remove the soot adjacent to the line of the Pt film. Colour analysis of the photocatalysed removal of soot revealed the following enhancement factor values: 0.063, 2.79 and 0.33 for the Ag-, Pt- and Au-TiO_2 films, respectively. Thus, similar experiments carried out using lines of the Ag and Au films showed no evidence for a

marked enhancement in activity, indeed, from an analysis of the associated photographic records of soot destruction as a function of irradiation time, the metal films appeared to impede the photocatalysed oxidation of the soot, see Table 1. Most notable of the values of δ is the value of 2.79 for the Pt/TiO_2 film, which was accompanied by the gradual appearance of a soot-free gap between the central Pt/TiO_2 line-shaped film and the soot on the adjacent TiO_2-only film. The appearance of such a gap is reminiscent of that observed by Choi et al [38], and this group [36], when irradiating soot-covered TiO_2 films on glass and which was ascribed to the spill-over of photogenerated, highly oxidising species, such as desorbed OH radicals [38]. Presumably something similar is responsible for the emerging gap illustrated in figure 7. It is not obvious why the Ag and Au films impede the photocatalysis of reaction (9), whilst, in contrast, the Pt film enhances it. However, these results suggest that, rather like the photocatalysed oxidation of CO, a very reactive oxygen species, O*, is generated on the Pt film, which is then able to oxidise the soot on the Pt and, by spilling-over, is then able to oxidise the soot on the adjacent TiO_2 film. These results and rationale provided suggest a connection between the photocatalysed oxidation of CO, discussed previously, and that of soot by the metal/TiO_2 films since, in both cases, Pt appears to enhance the reaction whereas both the Ag and Au films depress it, as indicated by the calculated values of δ for both reactions given in Table 1.

One other example of the photocatalytic oxidation of a solid material on a TiO_2 and Pt/TiO_2 was carried out, namely that of stearic acid, SA, i.e.

$$CH_3(CH_2)_{16}CO_2H + 26O_2 \longrightarrow 18\,CO_2 + 18H_2O \qquad (10)$$

This reaction is very popular in photocatalytic research since: (a) SA is a basic component of candle wax and provides a reasonable model compound for the solid films that deposit on exterior and interior surfaces, (b) SA is very stable under UV illumination in the absence of a photocatalyst film and (c) the kinetics of removal of SA are usually zero-order, and so SA film thickness is not usually a critical factor. Thus, in this work, samples of a TiO_2 sol-gel film with, and without, a covering of Pt were coated with SA using a dip-coating technique (0.1 M stearic acid solution in chloroform, immersion time: 1 s, withdrawal speed 100 cm min^{-1} [41,42]); the resulting stearic acid film had an integrated area between 2700–3000 cm^{-1} of 10.5 cm^{-1}, corresponding to a loading of 1.02×10^{17} molecules cm^{-2} [41].

When each sample was irradiated with UVA (2 mW cm^{-2}), the disappearance of the SA, *via* the photocatalysed reaction (10), was monitored using FT-IR absorption spectroscopy, since SA absorbs strongly in the region 2700–3000 cm^{-1}. From the absorbance versus irradiation time plots for each of the photocatalyst films the half-lives for the photocatalysed destruction of SA by the Pt/TiO_2 and TiO_2 films were determined and an enhancement factor of 0.77 calculated (see Table 1). The latter result suggests that the presence of Pt appears to depress the rate of reaction (10) compared to that of TiO_2 alone. This is possibly not too surprising given that the

proposed usual role of Pt in reaction (1) is to enhance the rate of O_2 reduction, i.e. reaction (2), compared to that of TiO_2 alone. In reaction (10), however, a solid film of SA covers both the TiO_2 and the Pt/TiO_2 making the diffusion of O_2 to the photocatalyst's surface, rather than its reduction, the more likely rate determining step; the latter feature would also explain why the observed kinetics are zero order with respect to SA thickness. In contrast, the soot covered TiO_2 and Pt/TiO_2 films would not be expected to show this effect since the soot films are fluffy, i.e. not solid wax coatings of SA, making O_2 diffusion facile and unlikely to be rate-determining.

Photocatalytic reduction: aqueous solution

The most common use of metal co-catalysts is to allow semiconductor photocatalysts to effect the reduction of water to H_2 in the absence of oxygen. In the case of free-standing photocatalysts, i.e. in powder or film form rather than in electrode form, almost always a sacrificial electron donor, such as glycerol is added to such systems, so that the overall reaction can be summarised as follows:

$$2SED + 2H^+ \xrightarrow[h\nu \geq E_{bg}]{TiO_2/M} 2SED^+ + H_2\uparrow \qquad (11)$$

In most examples of the semiconductor photocatalysed reduction of water, a metal co-catalyst, M, is essential since the overpotential for water reduction on most 'naked' semiconductors is very high. Indeed, at reduction potentials lower than that for water reduction, the Ti(IV) in TiO_2 is more likely to be reduced, to blue-coloured TI(III), than water.

Many different SEDs have been used in the past, including: coal, aliphatic hydrocarbons (e.g. pentane), aromatics (e.g. phenol), alcohols (e.g. ethanol), carbohydrates (e.g. glucose), proteins (e.g. gelatin), fatty acids (e.g. olive oil) and natural products, such as: cherry wood, rice plant, seaweed, cockroaches and cow manure [43]. However, the most popular SEDs for promoting the photocatalysed reduction of water are methanol and ethanol [43].

In order to demonstrate the effectiveness of the metal-coated TiO_2 films reported here, to mediate reaction (11), compared to the metal-free, i.e. naked, TiO_2 sol-gel film, each of the M/TiO_2 films illustrated in figure 1, along with a naked TiO_2 sol-gel film were, in turn, placed in a gas-tight cell containing 20 cm^3 of a 50:50 mixture (by volume) of an 0.02 M HCl aqueous solution and ethanol, respectively. Note: working under acidic conditions helps favour water reduction by shifting the band positions of the TiO_2 [44]. Each film was then irradiated for 1 h using a 200 W Hg-Xe lamp, with a UV irradiance of 12 mW cm^{-2}, and the amount of H_2 released into the headspace monitored, *via* GC, as a function of time. The results of this work are illustrated in figure 8, in the form of a plot of the total amount of H_2 generated as a function of irradiation time for the Ag-, Pt-, Au-TiO_2 and naked TiO_2 films.

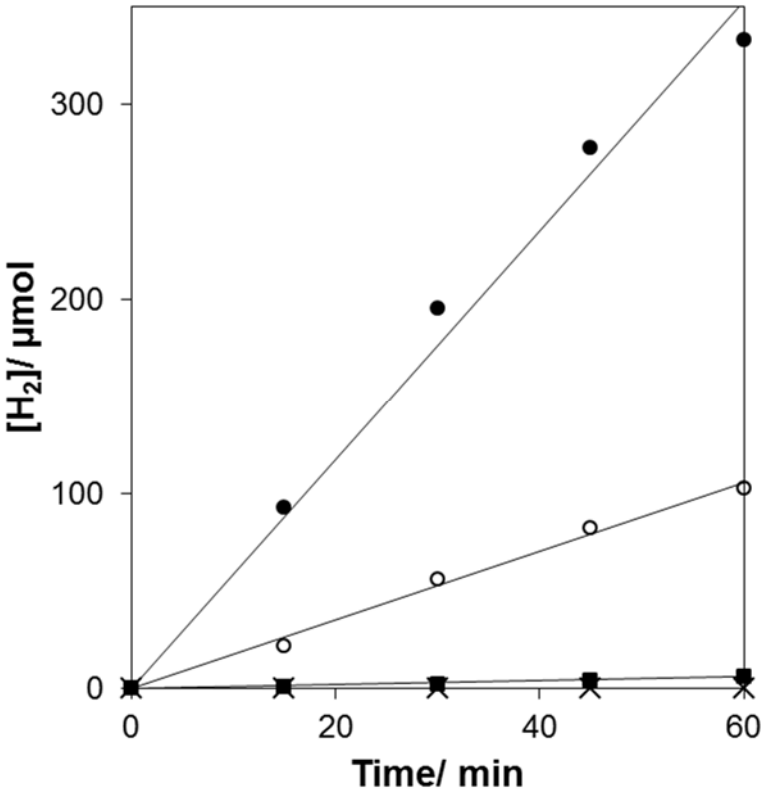

Figure 8: Plot of the total amount of H_2 generated as a function of irradiation time for reaction (11), where SED = ethanol. The reaction solution used was a 50:50 mixture (by volume) of 0.02 M HCl a Pt-TiO_2, and ethanol. The photocatalyst films used were (from top to bottom): Pt-TiO_2 (●), Au-TiO_2 (○) and Ag-TiO_2 (■). Note: the naked TiO_2 sol-gel film (x) did NOT generate any H_2.

From these results, the order of activities, with respect to reaction (11), for the different photocatalytic films tested was found to be: Pt-TiO_2 > Au-TiO_2 >> Ag-TiO_2, with the naked TiO_2 sol-gel film exhibiting no activity, see Table 1. As a consequence, the enhancement factors listed in Table 1 for reaction (11) are with respect to the Ag-TiO_2, rather than the naked TiO_2, film. The order of activities for the different films is the same as that for the reported exchange current densities for water reduction on these metals, i.e. 1.4×10^{-8}, 7.9×10^{-4} and 4.0×10^{-6} A cm^{-2} for Ag, Pt and Au respectively [45]. These results are consistent with the usual observation that the order in photocatalytic activities for water reduction observed for metal-coated TiO_2 photocatalysts reflects the different abilities of the metals to mediate the reduction of water by the photogenerated electrons, while the photogenerated holes are scavenged by the easily oxidised ethanol SED [43].

Conclusions

The photodeposition of Ag, Pt and Ag onto many commercial TiO_2 based photocatalytic materials, such as paint, tile, awning fabric and glass, as well as a TiO_2 sol-gel film, occurs readily using salts of the metals dissolved in an aqueous ink containing a sacrificial electron donor, glycerol. The rate of deposition of Ag is particularly fast, since only a 10 s irradiation, with 2 mW cm^{-2} UVA, is needed to produce a noticeable colour change, which is 60 times faster than the other two metal-ion containing inks. This high rate suggests that the Ag ink could be used as a fast-acting, photocatalyst activity indicator ink, especially for low activity surfaces, such as Hydrotec™ tiles for example [18]. When combined with a photomask, the metal inks can be used to create finely detailed metal film images on the surfaces of a range of photocatalytic films and, with an appropriate photomask, be used to make metal micro-patterns. The enhancement in photocatalytic activity exhibited by a Pt-coated TiO_2 film is modest (16-35%) for the photocatalysed oxidation of organic pollutants dissolved in aqueous solution, such as 4CP and MB. In contrast, the same film improves markedly the measured activity for the photocatalysed oxidation of CO to CO_2 (δ = 3.11); in contrast, the Au and Ag films have a negative effect. The Pt/TiO_2 film also enhances significantly the photocatalysed oxidation of a film of soot (δ = 2.79) but not of stearic acid (δ = 0.77). The most significant enhancement effect was observed using the Pt/TiO_2 film to promote the photocatalysed reduction of water to H_2 by ethanol (δ = 62), although the Au/TiO_2 film was also impressive (δ = 19), when compared to the very modest performance of the Ag/TiO_2 film. Overall, metal-ion containing inks appear a useful, simple approach to photodeposit metal films onto the surface of a wide number of different (TiO_2- based) photocatalytic materials.

References

[1] Sto, http://www.sto-sea.com/en/company/innovations/sto-climasan-color/sto-climasan-color-.html (Accessed May 2018).

[2] Pilkington, https://www.pilkington.com/en-gb/uk/householders/types-of-glass/self-cleaning-glass (Accessed May 2018).

[3] S-K. Lee, A. Mills, J. Ind. Eng. Chem. 10 (2004) 173–187.

[4] J. A. Byrne, P. A. Fernandez-Ibanez, P. S.M. Dunlop, D.A. Alrousan, and J.W. J. Hamilton, *Int. J. Photoenergy* (2011) 1–12.

[5] K. Wenderich, G. Mul, Chem. Rev. 116 (2016) 14587–14619.

[6] S-K. Lee, A. Mills, Platin. Met. Rev. 47 (2003) 61–72.

[7] A. Mills, J. Chem. Soc. Chem. Commun. (1982) 367–368.

[8] C. Xi, Z. Chen, Q. Li, Z. Jin, J. Photochem. Photobiol., A 87 (1995) 249–255.

[9] J. Lee, W. Choi, J. Phys. Chem. B 109 (2005) 7399–7406.

[10] H. Nakamatsu, T. Kawai, A. Koreeda, S. Kawai, J. Chem. Soc., Faraday Trans. 1 82 (1985) 527–531.

[11] F. Zhang, J. Chen, X. Zhang, W. Gao, R. Jin, N. Guan, Y. Li, Langmuir 20 (2004) 9329−9334.

[12] X.Jiang, X. Fu, L. Zhang, S. Menga and S. Chen, J. Mater. Chem. A 3 (2015) 2271–2282.

[13] A. Mills and N. Wells, *Chem. Soc. Rev*. 44 (2015) 2849–2864.

[14] https://en.wikipedia.org/wiki/Photocatalyst_activity_indicator_ink (Accessed May 2018).

[15] A. Mills, *Appld. Catal. B* 128 (2012) 144–149.

[16] ISO/DIS 21066, https://www.iso.org/obp/ui/#iso:std:iso:21066:dis:ed-1:v1:en (Accessed May 2018)

[17] A. Mills, N. Wells, C. O'Rourke, *Catal. Tod.* 230 (2014) 245–249.

[18] Deutsche Steinzeug, https://www.deutsche-steinzeug.de/en/news/presse_und_news_detail.html?nd_ref=1497

[19] Mitsubishi Paper Mills, https://www.mpm.co.jp/eng/rd/field/functional-material.html (Accessed May 2018).

[20] St. Gobain, https://www.sheerfill.com/document/sheerfill-ultralux-everclean-astm-datasheet (Accessed May 2018).

[21] Pilkington, http://www.pilkington.com/en/global/products/product-categories/self-cleaning/pilkington-activ-range (Accessed May 2018).

[22] A. Mills, N. Elliott, G. Hill, D. Fallis, J.R. Durrant, R.L. Willis, Photochem. Photobiol. Sci. 2 (2003) 591–596.

[23] M. Rycenga, C. M. Cobley, J. Zeng, W. Li, C. H. Moran, Q. Zhang, D. Qin, Y. Xia, Chem. Rev. 111 (2011) 3669–3712.

[24] C. Y. Wang, C.Y. Liu, J. Chen, T. Shen, Colloid. Surf. A 131 (1998) 271–280.

[25] M. Hiramoto, K. Hashimoto, T. Sakata, Chem. Letts. (1986) 899–902.

[26] H. Sugimura, T. Ucida, N. Kitamura, H. Masuhara, Chem. Letts. 22 (1993) 379–382.

[27] S. Juodkazis, H. Ishii, S. Matsuo, H. Misawa, J. Electroanal. Chem. 473 (1999) 235–239.

[28] T. Inoue, AS. Fujishima, K. Honda, J. Electrochem. Soc., 127 (1980) 1582–1588.

[29] Wikipedia, https://en.wikipedia.org/wiki/Samson_and_Goliath_(cranes) (Accessed May 2018).

[30] A. Mills, N. Wells, C. O'Rourke, *J. Photochem. Photobiol. A* 330 (2016) 86–89.

[31] H. Einaga, M. Harada, S. Futamura, T. Ibusuki, J. Phys. Chem. B 107 (2003) 9290–9297.

[32] S. Hwang, M. Churl Lee, W. Choi, Appl. Catal. B 46 (2003) 49–63.

[33] M. Gajdoš, A. Eichler, J. Hafner, J. Phys. Condens. Matter 16 (2004) 1141–1164.

[34] A. Mills, S. Elouali, J. Photochem. Photobiol. A 305 (2015) 29–36.

[35] A. Mills, C. Hill, P.K.J. Robertson, J. Photochem. Photobiol. A 237 (2012) 7–23.

[36] S. K. Lee, S. McIntyre, A. Mills, J. Photochem. Photobiol. A 162 (2004) 203–206.

[37] A. Mills, J. Wang, M. Crow. Chemosphere 64 (2006) 1032–1035.

[38] M.C Lee, W. Choi, J. Phys. Chem. 106 (2002) 11818–11822.

[39] P. Chin, C. S. Grant, D. F. Ollis, Appl. Catal. B 87 (2009) 220–229.

[40] T. R. Knutson, C. M. Knutson, A. R. Mozzetti, A. R. Campos, C. L. Haynes, R. L. Penn, J. Chem. Educ. 92 (2015) 1692–1695.

[41] A. Mills, J. Wang, J. Photochem. Photobiol. A 182 (2006) 181–186.

[42] R. Quesada-Cabrera, A. Mills, C. O'Rourke, Appl. Catal., B 150– 151 (2014) 338–344.

[43] T. Sakata T. Kawai, Photosynthesis and photocatalysis with semiconductor powders, in 'Energy Resources through photochemistry and catalysis', M. Gratzel, Academic Press, 1983, Chapter 10, pp. 331–358.

[44] P. Carmichael, D. Hazafy, D. S. Bhachu, A. Mills, J. A. Darr, I. P. Parkin, Phys.Chem. Chem. Phys. 15 (2013) 16788–16794.

[45] J.K. Norskov, T. Bligaard, A. Logadottir, J.R. Kitchin, J.G. Chen, S. Pandelov and U. Stimmings, J. Electrochem. Soc. 152 (2005) J23–J26.